GRAIN LEVEL ANALYSIS OF CERAMIC MICROSTRUCTURES SUBJECTED TO IMPACT LOADING

Pablo D. Zavattieri and Horacio D. Espinosa
Mechanical Engineering, Northwestern University, Evanston, IL 60208

ABSTRACT

A study on the accuracy of cohesive models for capturing dynamic fragmentation of ceramic microstructures is presented. The investigation consists of a combined experimental/numerical approach in which microcracking and damage kinetics are examined by means of plate impact recovery experiments. The numerical analysis is based on a 2-D micromechanical stochastic finite element analysis. The model incorporates a cohesive law to capture microcrack initiation and evolution as a natural outcome of the calculated material response. Normal plate impact velocity histories are used not only to identify model parameters, but also to determine under what conditions the model captures failure mechanisms experimentally observed. The analyses show that in order to capture damage kinetics a particular distribution of grain boundary strength and detailed modeling of grain morphology are required.

1. INTRODUCTION

Critical elements in the development of a physically-based model of the dynamic deformation and failure of ceramics requires experiments specifically designed to examine inelasticity. For instance, to study the initiation and evolution of microcracks in ceramics, an experiment that can cause controlled microcracking, under well defined stress conditions, was developed by Clifton and co-workers [1, 2]. These investigators performed plate impact *soft recovery* experiments by subjecting the central region of a square ceramic specimen to known and controllable stress pulses. Microcracking resulted yet the specimens were recovered intact for microscopic analysis.

A large portion of the microcracks was found to originate at triple points and both inelasticity in compression and tension was interferometrically measured. In the tension dominated region, several microcracks linked together to form a spall plane perpendicular to the impact direction. In spite of these contributions to the field of damage, lack of consensus on the mechanisms responsible for ceramic failure under multi-axial dynamic loading still remains.

Attempts have been made to model the inelastic constitutive behavior of ceramics in the presence of cracks, and to validate the models through simulation of plate and rod impact experiments. Available models for the failure of ceramics are continuum damage theories which are based on homogenizing the cracked solid and finding its response by degrading the elasticity of the material, and discrete approachs [3, 4], able to nucleate cracks, and follow their propagation and coalescence during the deformation process, the influence of microscopic heterogeneities on the overall material behavior, which depends on morphological characteristics such as size, shape, lattice orientation and spatial distribution of grains, is not accounted for.

In order to provide powerful tools to understand the mechanisms that lead to macroscopic failure and, at the same time, refine the theories of damage utilized in continuum or continuum/discrete models, a 2-D micromechanical model is presented to assess intergranular microcrack initiation and evolution. A representative volume element (RVE) of an actual microstructure, subjected to multi-axial dynamic loading, is considered for the different analyses. A large deformation elastic-anisotropic visco-plasticity model for the grains, incorporating grain anisotropy by randomly generating principal material directions, is included. Cohesive interface elements are embedded along grain boundaries to simulate intergranular fracture through microcrack initiation and evolution. Their interaction and coalescence are a natural outcome of the calculated material response.

This micromechanical model provides explicit account for arbitrary microstructural morphologies and microscopic fracture patterns making it easier to identify and design microstructural configurations that enhance fracture toughness, and therefore lead to improvements in the manufacturing of ceramic materials. A detailed study of the damage initiation and kinetics in *soft-recovery* experiments is carried out.

The objective of this work is to provide tools and means to understand the macroscopic inelastic response of ceramics when subjected to dynamic multiaxial loading at the micron scale. This bridging between scales is achieved by a micro-mechanical stochastic finite element model. Experiments are not only used to examine and validate the micromechanical model but also to explain the different failure mechanisms.

2. MICROMECHANICAL MODEL

The finite element analysis of the initial boundary value problem is per-

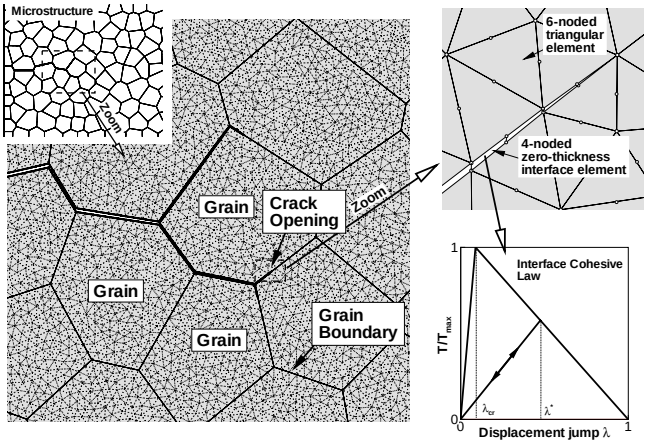

(a)

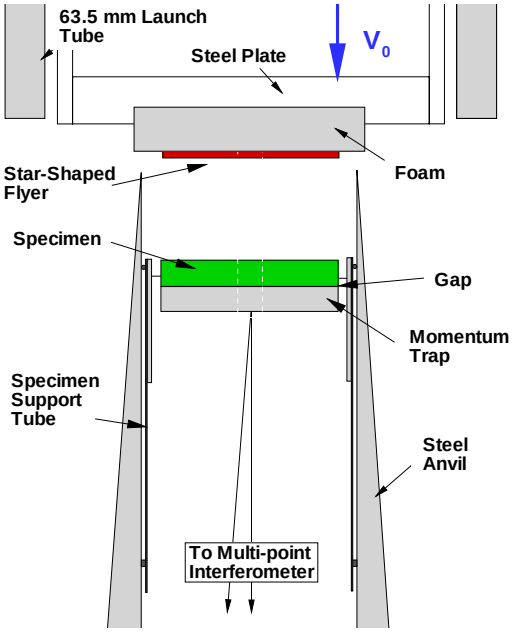

(b)

Figure 1: (a) Schematics of microcracking at grain boundaries using an irreversible interface cohesive law. (b) Soft-recovery normal impact configuration.

formed using a total Lagrangian continuum approach with a large deformation elastic and thermal anisotropic visco-plastic model [5, 6]. The elastic and thermal anisotropic model is used to describe grains' single crystal anisotropic behavior. Each grain is assumed to be elastic orthotropic and the orientation of the principal material directions differs from grain to grain.

A multi-body contact-interface algorithm is used to describe the kinematics at the grain boundaries and to simulate crack initiation and propagation. Figure 1 describes the contact model, integrated with interface elements to simulate microcracking at the grain boundaries and subsequent large sliding, opening and closing of the interface. The tensile and shear tractions in the zero thickness interface elements, embedded along grain boundaries, are calculated from the interface cohesive law. The interface cohesive law describes the evolution of these tractions in terms of both normal and tangential displacement jumps. Within the framework of cohesive interface elements the two most noteworthy cohesive failure models available in the literature are the potential-based law [7], and the linear law [3]. More detail on the cohesive model used in this work can be found in the following references [5, 6].

3. SOFT-RECOVERY IMPACT EXPERIMENTS

The *"soft-recovery"* plate impact experiment has been described in detail by Raiser et al. [1], and Espinosa et al. [2]. The experiment uses an eight pointed start-shaped flyer plate that impacts a square ceramic specimen, subjecting the central octagonal region to a plane pulse. Figure 1(b), shows this soft-recovery normal impact configuration. A tensile pulse is originated from a gap between the specimen and the momentum trap upon reflection of the compressive pulse. The velocity-time profiles recorded at the rear surface of the momentum trap plate provide information on microcrack initiation and evolution.

Let x denote the distance from the front surface of the specimen measured in the direction of impact, and let L_s denote the thickness of the specimen, L_f the thickness of the flyer and L_{MT} the thickness of the momentum trap. The particle velocity induced in the rear surface of the momentum trap is measured as a function of time by a normal displacement interferometer (NDI) and a normal velocity interferometer (NVI).

In the case of brittle materials readily damaged in tension, the tensile region becomes the likely site of substantial damage called *spall region*. When spallation initiates, the release waves emitted from the newly created free

surfaces completely change the pattern of waves inside the specimen. The shape of the pull-back signal and second compressive pulse reflects both microcracking, under the tensile pulse itself, and attenuation while traveling through material already damaged. The above one-dimensional analysis is valid in the central region of the specimen, where the effects of diffracted waves from the corners and the edges of the flyer are minimized [2]. The experimental findings suggested that the modeling of crack nucleation and growth requires consideration not only of the amplitude of the applied stress but also of its time dependence [2]. Several successful tests have been conducted using this experimental design by Espinosa et al. [2] and Raiser et al. [1]. A summary of the shots used for comparisons with the proposed numerical model can be found in Zavattieri and Espinosa [8].

4. STOCHASTIC FEM SIMULATIONS

A representative volume element of an actual microstructure is considered for the analysis. Although the exact grain geometry can be taken from a digital micrograph, it is well established that the grain structure in polycrystalline materials can be simulated by a Voronoi tessellation [6]. We followed the last approach to generate enough statistical data.

Figure 2(a) shows a strip of the various plates used in the experimental configuration, only the flyer, momentum trap and specimen are considered in the analysis and due to the limited spread of tensile damage observed experimentally, only a small portion of the ceramic in the spall region is simulated. The top and bottom boundaries of the cell are modeled using viscous boundary conditions which represent the exact elastic wave solution along characteristic lines. Details on the boundary conditions and convergence can be found in [6].

5. ANALYSIS OF THE SOFT-RECOVERY IMPACT EXPERIMENTS

In order ot simulate these experiments, two important features were incorporated in the simulation of the experiments, namely, (1) a Weibull distribution of the interfacial strength and fracture toughness along the grain facets and (2) realistic microstructures considering grain morphology and size distributions.

As discussed in [5, 6, 8], it is physically incorrect to select a uniform T_{max} and K_{IC} for all grain facets. Not only that grain misorientation affect the interfacial strength, but also it affect the presence of glassy phase, glass

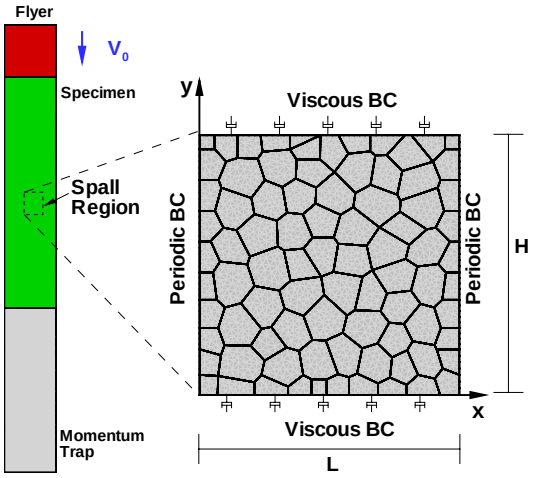

(a)

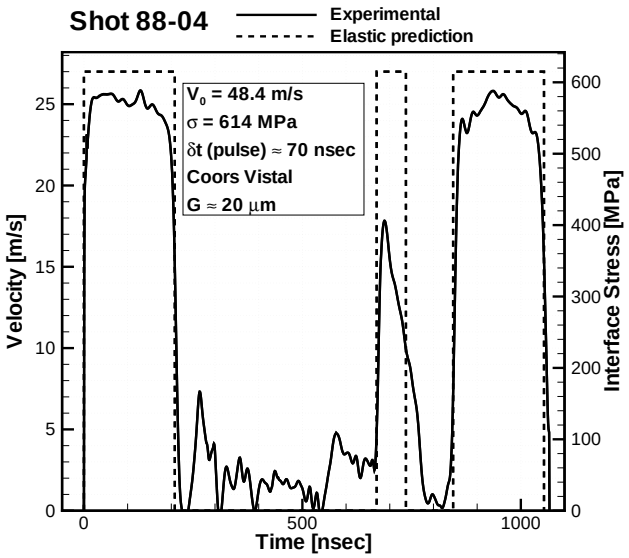

(b)

Figure 2: (a) Schematics of the computational cell used for the analyses. (b) Experimental particle velocity versus time for one (Shot 88-04) of the experiments performed by Espinosa et al. [2].

pockets, and other impurities that modify grain boundary properties. In the following analyses, the interfacial strength parameters will be described by a *Weibull* distribution.

5.1. Simulation of experiment 88-04

Figure 2(b) shows the experimental particle velocity vs time for Shot 88-04 performed by Espinosa et al. [2]. The impact velocity used in Shot 88-04 was $V_0 = 48.4m/s$. Figure 2(b) shows the experimental velocity history for this experiment. The elastic solution is also shown in the same figure. The most significant features of this experiment is the pullback signal (almost 30% of the maximum stress) and the spreading of the second compressive pulse. Numerical simulations using the microstructure shown in Figure 2(a) result in a pull-back signal with a maximum stress equal to the first compressive pulse, which is well above the pull-back signal measured experimentally. Once microcracks nucleate, they grow at rates such that a major crack from side to side of the RVE develops. It is worth noticing that even for the case in which there is only one nucleation site every 200 μm, the crack has to propagate to the other side of the RVE, in more than 67 nanoseconds (tensile pulse duration), in order to have a pullback signal below 100 % of the compressive pulse. This would require a crack speed of less than 50% of the Rayleigh wave speed, which for alumina is 3 $mm/\mu s$, or a delay in the decohesion process produced by rate effects. From the SEM Micrographs [2], it is observed that the microcracks need to follow grain boundaries, with large variations in grain size. The net effect is that crack propagation speed on a projected horizontal plane is reduced to a fraction of the Rayleigh wave speed. We closely examine this feature in conjunction with the observation of possible nucleation sites as a function of overstress from the threshold level.

Two microstructures are considered in this analysis. Both meshes have a width of 300 μm such that if there is only one nucleation site, the crack will have a total time equal to the pulse duration to coalesce into a main crack. The main idea of this analysis is to compare *vis-à-vis* the crack propagation for two different types of microstructures: Microstructure **A**, with a non-uniform distribution of grain sizes and shapes (motivated from the micrographs), and microstructure **B** with a uniform distribution of grains (all with the same size and similar shape). Figure 3(a) shows in detail the pullback signal for simulations considering microstructure **A**. Microstructures **A** and **B** are shown in Figure 4. In these simulations three different

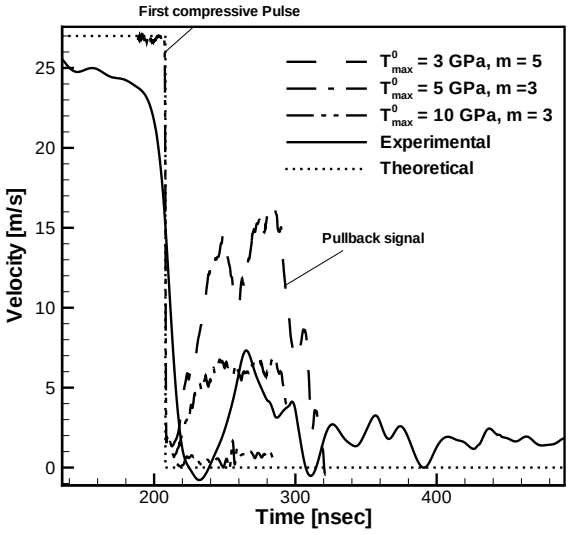

(a)

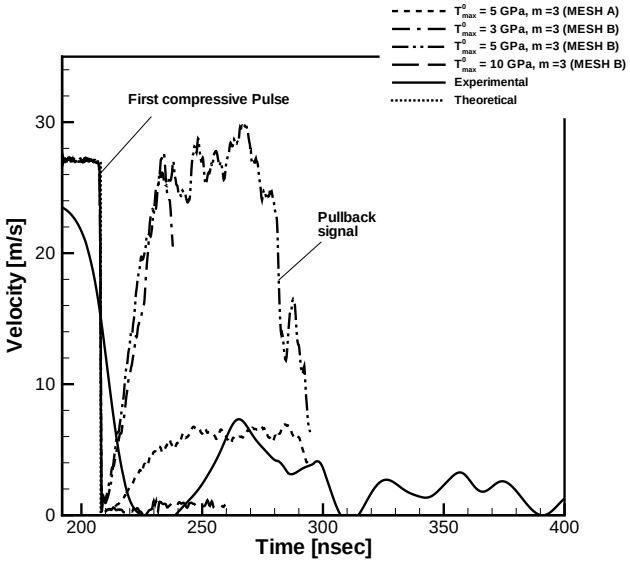

(b)

Figure 3: (a) Comparison between three different Weibull distribution for Shot 88-04 using mesh A. (b) Comparison between the velocity history using meshes A and B.

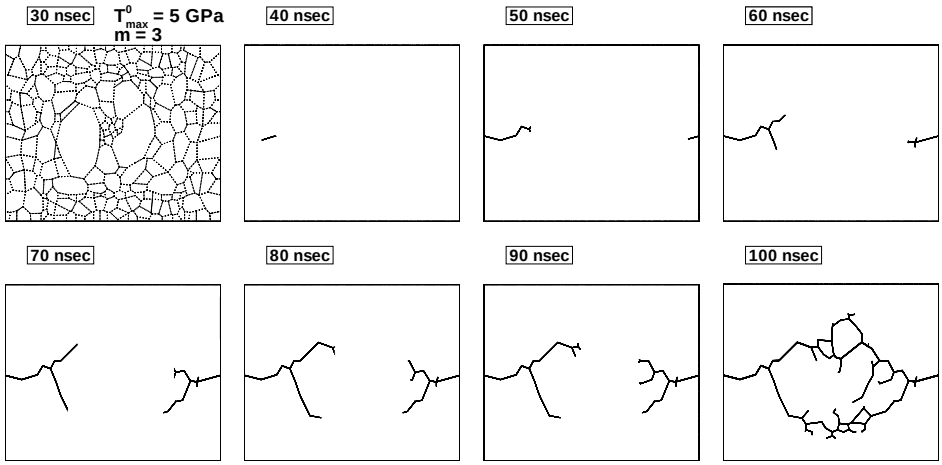

(a)

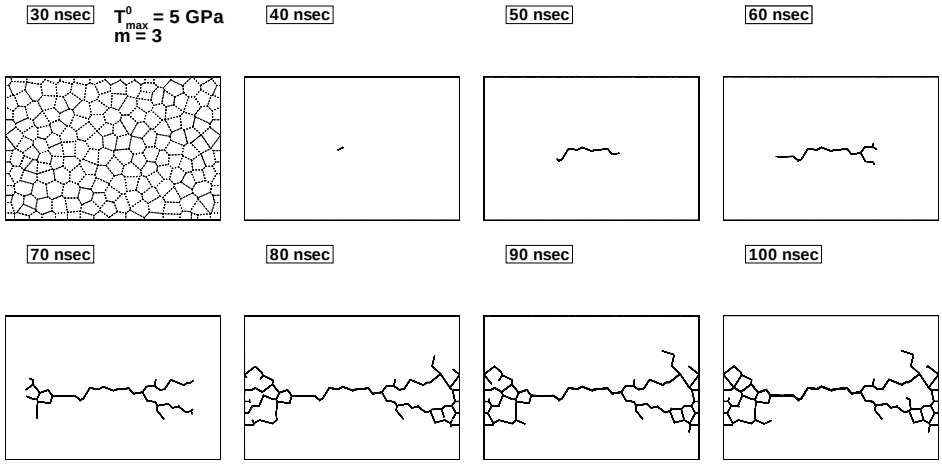

(b)

Figure 4: (a) Evolution of crack pattern for the case with $T^0_{max} = 5$ and $m = 3$ using mesh A. (b) Evolution of crack pattern for the case with $T^0_{max} = 5$ and $m = 3$, using mesh B.

Weibull distributions have been considered. The best fit is obtained for a Weibull distribution with $T^0_{max} = 5$ GPa, $K^0_{IC} = 2$ MPa $\cdot$ m$^{1/2}$ and $m = 3$. This distribution contains interface elements with $T_{max} = 0.5$ GPa and $T_{max} \approx 10GPa$. The same distributions have been considered for microstructure **B**, see Figure 3(b), and the pullback signals are much more pronounced than those obtained with microstructure **A**. An explanation can be inferred by examining the evolution of crack patterns as shown in Figure 4. The evolution of the microcracks for $T^0_{max} = 5$, $K^0_{IC} = 2$ MPa $\cdot$ m$^{1/2}$ and $m = 3$ using mesh A is shown in Figure 4(a); the grain morphology is shown in the first frame. In this case, it can be observed that the microcracks need to go around the large grains at the center of the RVE. The time that it takes the crack to surround the large grains is similar to the pulse duration and then the pullback signal is significantly lower than for cases where the crack propagates, from one side to the other of the RVE, at uniform speed. Figure 4(b) shows the crack evolution for the case with microstructure **B**. The crack initiates almost in the middle of the RVE and propagates at constant speed until it coalesces into a main crack just before the tensile pulse vanishes. As a result, the pullback signal for this case is much higher than that for the case where the crack is forced to follow a path around large grains.

5.2. Higher impact velocities

In this subsection we examine an experiment with higher impact velocity. The experiment (Shot 92-11) has been reported by Raiser et. al [1], the initial velocity was $V_0 = 92.3m/s$. The main variation in this experiment is the average grain size of the ceramic, Coors AD-999, of approximately 3 μm. For this analysis an RVE of $200 \times 200\mu m$ is considered and two type of microstructures, uniform and bi-modal grain sizes, are analyzed. The main motivation for examining two different microstructures is to study the effect of grain morphology and how this affect the crack path and crack speed along the spall plane. Although the second microstructure with a bi-modal distribution of grain sizes may not be totally representative of the tested ceramic, it is used to evidence the effect of grain morphology.

An analysis with three different Weibull distribution on the RVE with uniform grain size has been carried out; weak interface case: $T^0_{max} = 3GPa$ and $m = 3$; the case considered in previous experiments, i.e., $T^0_{max} = 5GPa$ and $m = 3$; and a strong interface case: $T^0_{max} = 10GPa$ and $m = 10$. The intention of this analysis is not to study parametrically the effect of m, or T_{max}

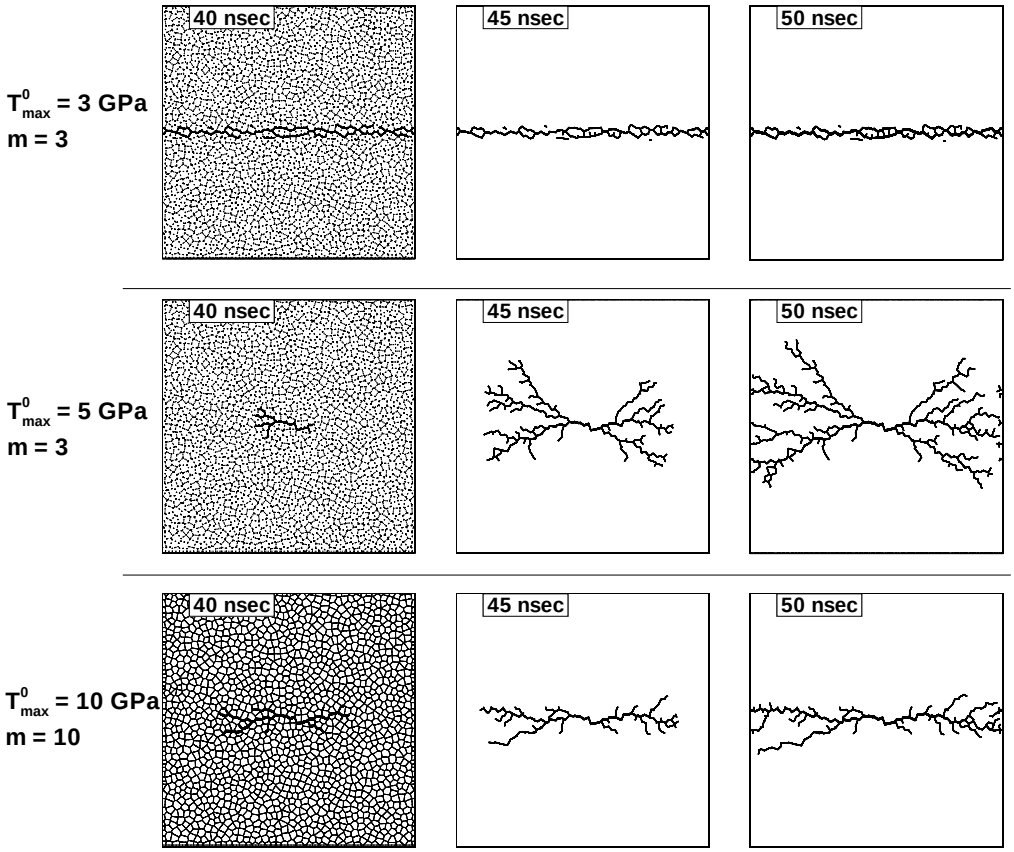

Figure 5: Velocity history for Shot 92-11 using a microstructure with a uniform distribution of grain size and three different Weibull distributions.

. In all cases K_{IC}= 2 MPam$^{1/2}$. Figure 5 shows the crack pattern for each one of these cases; the grain morphology is shown in the first frame. In the weak interface case, the ceramic fails from side to side right after the tensile pulse is generated at the spall plane. Crack nucleation occurs basically at a large percentage of triple points and coalescence of microcracks occurs before the end of the tensile pulse. For the case with $T^0_{max} = 5GPa$ and $m = 3$ the crack start propagating from the center to the borders and crack branching in the form of a *"funnel"* is observed. As it is expected, the strongest case ($T^0_{max} = 10GPa$ and $m = 10$) shows less branching and microcrack density. The energy to create new surfaces is higher so that branching is inhibited.

6. DISCUSSION

The micromechanical analyses, together with the experimental velocity profiles and SEM observations, have demonstrated that there are two factors to be taken into account to capture the right damage kinetics occurring during the experiments. In view that not all grain facets have the same interface strength and local fracture toughness, it is important to consider Weibull distributions of T_{max} and K_{IC} . Similarly, since the ceramic microstructures interrogated in these experiments do not contain grains with the same shape and size, microstructures with non-uniform distributions of grain size and shape must be considered. On the other hand, microstructures with non-uniform distribution of grain size and shape strongly affect crack speed along the spall plane.

From a computational standpoint, simulations of ballistic penetration, vehicle crash analysis, manufacturing processes, etc. cannot be conducted at the grain level. Hence, this fundamental study of brittle failure provides insight into the utilization of cohesive laws at other size scales. Our simulations clearly show that the scale at which simulations are performed plays an important role in the selection of cohesive models. The calculations in this work make assumptions that limited the degree of achievable accuracy. For instance, the model is two-dimensional and crack interaction is stronger than in the 3-D case and therefore, the computed rate of crack coalescence may be thought of as an upper bound. Despite these limitations, the numerical results obtained with this model were not only in good agreement with the experiments, but also were used to explain several microscopic failure mechanisms that have never been quantified before through other mathematical models.

7. REFERENCES

[1]Raiser G., Wise J.L., Clifton R.J., Grady D.E., and Cox D.E., "Plate impact response of ceramics and glasses", *J. Appl. Phys*., 75(8):3862-69,1994.

[2]Espinosa H.D., Raiser G., Clifton R.J., and Ortiz M., "Experimental observations and numerical modeling of inelasticity in dynamically loaded ceramics", *J. Hard. Mat*., 3:285-313, 1993.

[3]Camacho G.T. and Ortiz M. "Computational modeling of impact damage in brittle materials", *Int. J. Sol. Str*., 33: 2899-2938, 1996.

[4]Espinosa H.D., Zavattieri P.D., and Dwivedi S., "A finite deformation continuum/discrete model for the description of fragmentation and damage in brittle materials", *J. of the Mechanics and Physics of Solids*, 46(10): 1909-1942, 1998.

[5]Zavattieri P.D., Raghuram P.V., and Espinosa H.D., "A computational model of ceramic microstructures subjected to multi-axial dynamic loading", *J. of the Mechanics and Physics of Solids*, 49(1): 27-68, 2001.

[6]H.D. Espinosa and P.D. Zavattieri, "A grain level model for the study of dynamic failure of polycrystalline materials. Part I: Theory and numerical implementation", Submitted to *Mechanics of Materials*, 2001.

[7]Xu X-P and Needleman A., "Numerical simulation of dynamic interfacial crack growth allowing for crack growth away from the bond line", *Int. J. Fra.*, 74:253-275, 1995.

[8]P. D. Zavattieri and H. D. Espinosa, "Grain level analysis of crack initiation and propagation in brittle materials", In press *Acta Materialia*, 2001.